Heterogeneous Charge Transfer at the Amorphous Carbon/Solution Interface: Effect on the Spontaneous Attachment of Aryldiazonium Salts

Deirdre M. Murphy, Ronan J. Cullen, Dilushan R. Jayasundara, Richard L. Doyle, Michael E. G. Lyons and Paula E. Colavita [*]

School of Chemistry, University of Dublin Trinity College, College Green, Dublin 2, Ireland.

Centre for Research on Adaptive Nanostructures and Nanodevices (CRANN), University of Dublin Trinity College, Dublin 2, Ireland

[*] Corresponding author. School of Chemistry, University of Dublin Trinity College, College Green, D2, Ireland. Tel: +353 1 8963562; E-mail: colavitp@tcd.ie.

Abstract

The chemisorption of aryldiazonium salts is one of the most versatile reactions for the modification of carbon surfaces; in this work we investigated the spontaneous chemisorption of aryldiazonium salts at amorphous carbons of differing graphitic content in order to relate surface reactivity to the valence electronic properties of aryldiazonium cations and carbon surfaces. Two structural isomers that differ by their redox potential were chosen for our studies: 4-Nitronaphthalenediazonium tetrafluoroborate (4NND) and 5-nitronaphthalenediazonium tetrafluoroborate (5NND). The adsorption of 4NND and 5NND was studied in situ via attenuated total internal reflectance Fourier Transform infrared spectroscopy (ATR-FTIR) and ex situ via electrochemistry on two types of graphitic amorphous carbons (a-C), containing 80% and 100% trigonally bonded carbon centers. These two forms of carbon were characterized via Electrochemical Impedance Spectroscopy (EIS) and the more graphitic surface was found to display a heterogeneous charge transfer rate constant two orders of magnitude larger than the less graphitic surface. This was consistent with Ultraviolet Photoelectron Spectroscopy (UPS) results showing that the density of occupied states near the Fermi level is higher for the more graphitic substrate. In situ and ex situ studies of adsorption rates show that, on the less graphitic a-C surface, differences in adsorption rate could be explained based on the reduction potentials of the two aryldiazonium cations. However, on the more graphitic surface we observed no difference in adsorption rates or yields between the two isomers, thus suggesting that spontaneous electron transfer is not rate determining at these surfaces. Gerischer-Marcus theory was used in order to explain the differences in charge transfer rates between the two carbons and to interpret observed differences in aryldiazonium adsorption rates at these substrates. Finally, our results are discussed in light of the current proposed mechanism of aryldiazonium chemisorption.

Keywords: aryldiazonium, polycyclic aromatic hydrocarbon, PAH, electron transfer, amorphous carbon, Marcus theory.

1. Introduction

The chemisorption of aryldiazonium salts at carbons is a versatile surface modification methodology that has found multiple applications in fields as diverse as bioimaging, electronic devices and sensors.[1-4] Aryldiazonium salts graft covalently to carbon surfaces via a reductive process that can either be triggered electrochemically or occur spontaneously from solution. The spontaneous attachment route is particularly advantageous because no electrical contact is required for the reaction to occur, thus allowing researchers to expand aryldiazonium reactions to the modification of nanomaterials in suspension and of substrates with low conductivity.[4,5] Therefore, there has been great interest in understanding the mechanism of this reaction at carbons in order to, in turn, improve control over structure, morphology and composition of resulting organic layers.

The spontaneous chemisorption reaction is thought to proceed via a first step in which electron transfer from the substrate to the aryldiazonium cation leads to the formation of a reduced adsorbate species. In a second step, the adsorbate undergoes dediazoniation leading to chemisorption via aryl—surface covalent bonds (see Scheme Ia).[6-9] Assuming reductive adsorption is rate determining, rates of reaction are expected to depend on the overlap between surface donor states and molecule acceptor states.[1] Experimental evidence that supports this proposed mechanism has been provided for spontaneous aryldiazonium grafting at ordered carbon nanomaterials such as nanotubes[8-11] and graphene.[1,7] Recently, work from our group has shown that the proposed mechanism can be used to rationalise reaction trends of carbon materials that do not display long range order, such as amorphous carbons. We have shown that when the electronic properties of amorphous carbon change from metallic to semiconducting, adsorption rates drop dramatically.[12] Conversely, molecular acceptor levels can strongly affect adsorption rates at amorphous carbons. For instance,[13] using in situ spectroscopy we showed that adsorption rates of 4-nitronaphthalene (4NND) and 5-nitronaphthalene (5NND) diazonium tetrafluoroborate, two positional isomers (see Scheme Ib), were remarkably different. These differences were explained on the basis of their reduction potential given that adsorption and chemisorption rates were faster for 4NND, the isomer that had a lower lying acceptor level, than for 5NND.[13]

Results in our previous work suggest that when a carbon surface is exposed to more than one aryldiazonium salt, diazonium cations will establish a kinetic competition for surface sites based on their reduction potential. Herein we show that it is possible to switch-off such competition by changing the electronic properties of the amorphous carbon substrate. We have used a combination of spectroscopic and electrochemical methods in order to characterize two amorphous carbon materials that differ by their degree of graphitization, and investigate their reactions in situ and ex situ with the two isomeric aryldiazonium cations 4NND and 5NND. To our knowledge this is the first time that a modification of electronic properties is shown to control relative reaction rates at the carbon/solution interface in disordered carbon materials. We discuss our results in light of our current understanding of aryldiazonium chemisorption reactions and available models of charge-transfer at the solid/liquid interface. In particular, we show that Gerischer-Marcus theory can be used to make semiquantitative predictions on charge transfer rates at amorphous carbons and we use this approach in order to interpret our experimental observations of relative adsorption rates.

2. Experimental Section

Chemicals and Materials. 4-Nitrobenzenediazonium tetrafluoroborate (4NBD, 97%), 4-nitrobenzylamine hydrochloride (97%), potassium chloride (99%), potassium ferricyanide (99+%), potassium nitrate (≥98%) hexaminеruthenium(III) chloride (98%), hexaminеruthenium(II) chloride (99%) and sulfuric acid (95-97%) were obtained from Sigma and used as received. Degassed deionized water was used for all aqueous solutions. 4-Nitronaphthalenediazonium tetrafluoroborate (4NND) and 5-nitronaphthalenediazonium tetrafluoroborate (5NND) were synthesized as described previously.[13] 4-Nitrobenzylamine (4NBA) was prepared from 4-nitrobenzylamine hydrochloride salt using published methods.[14]

Preparation of carbon substrates. Amorphous carbon films with thicknesses in the range 40-50 nm were prepared via DC-magnetron sputtering (Torr International, Inc.) at a base pressure $\leq 2 \times 10^{-6}$ mbar

and a deposition pressure of 7×10^{-3} mbar, as previously described.[12] Sputter-coating was performed on silicon for infrared, Raman and photoelectron spectroscopies, on quartz slides (UQG Optics) for UV−vis measurements and on glassy carbon (GC) substrates for electrochemical measurements. GC substrates (SPI-Glas™ 11 Grade) were polished with 0.3 μm alumina slurry (Buehler), rinsed with water, immersed for 20 s in piranha to remove the polishing debris layer and rinsed with abundant water.[15] Annealing was carried out in a tube furnace at 500°C and 700°C for 1 hr under N_2 atmosphere.

Functionalization of carbon substrates. In situ real time analysis of the spontaneous grafting of 1×10^{-4} M solutions of aryl diazonium salts onto carbon substrates was monitored using a custom built ATR-FTIR, as previously reported.[12,13] Spectra were obtained at regular times upon commencement of reaction of using a Bruker Tensor 27 FTIR; 100 scans at 4 cm^{-1} resolution were averaged for each measurement over 3 h. The symmetric N—O stretching peak (1342 cm^{-1}) was chosen for the analysis because it was less affected by interferences from water vapor peaks than the asymmetric stretching peak (~1530 cm^{-1}). Spectra were normalized for optical pathlength using a 0.2 M aqueous KNO_3 solution, and for absorption cross section using an internal standard method, as previously described.[13] Aryldiazonium grafting on GC substrates was carried out via immersion in aqueous solutions of the salt for varying lengths of time. The substrates were washed, sonicated in water and dried under an Ar flow prior to electrochemical analysis.

Characterization. Raman spectra were obtained using the 514 nm line of an Ar^+ laser on a micro-Raman system (Renishaw 1000) equipped with a CCD camera and a Leica microscope with 1 cm^{-1} spectral resolution. In order to obtain I_D/I_G ratios, peaks were fitted using a combination of a Breit-Wigner-Fano and a Lorentzian peak[16] using commercial software (Igor Pro 6.04). UV−vis transmission measurements of amorphous carbon films were collected over the wavelength range 200−890 nm at 1 nm resolution (Shimadzu UV-2401 PC) from carbon samples deposited on quartz substrates. X-ray and Ultraviolet photoelectron spectroscopy (XPS and UPS) measurements of carbon substrates were carried out in an Omicron system with a multichannel array detector, at 1×10^{-10} mbar base pressure. XP spectra

were recorded at room temperature at 45° take-off angle with an analyzer resolution of 0.5 eV using a monochromatized Al K_α source (1486.6 eV). Peaks were fitted to Voigt functions after Shirley background correction, using commercial software (Igor Pro 6.04). UPS spectra were taken using a He(I) line as an excitation source, a take-off angle of 90° and an analyzer resolution of 0.02 eV. Measurements were collected by applying a negative bias to the sample in order to measure the high binding energy edge of the photoelectron spectrum. Spectra were corrected for bias and referenced to the Fermi energy, as measured from the Fermi step of a copper clip in electrical contact with the carbon substrates.[17] In order to compare spectra of different carbon samples, curves were normalized by the total integrated intensity for binding energies greater than 11.0 eV;[18] relative spectral intensities near the Fermi energy were found to be similar when the normalization was carried out using the full energy range. The work function was calculated from the difference between the incident photon energy (21.2 eV) and the energy cutoff at high binding energy. The cutoff value was determined from the intercept of linear fits of the spectrum before and after the emission threshold.[19,20]

Atomic Force Microscopy (AFM) measurements were carried out to characterize the roughness of the carbon surfaces before and after modification with aryldiazonium salts, followed by a light water rinse, as previously described.[21] AFM measurements were carried out in tapping mode with a frequency of 1 Hz and 512 scan lines; root-mean-square (RMS) roughness values were calculated over 2 × 2 μm^2 boxes with measurements carried out in triplicate. Electrochemical measurements were carried out in a home built Teflon cell in which the carbon substrate was utilized as the working electrode (0.067 cm^2), with a Pt wire and Ag/AgCl (IJ Cambria) acting as counter and reference electrodes, respectively. Cyclic voltammetry measurements were obtained on a CHI660C potentiostat at room temperature in Ar-purged 0.1 M H_2SO_4 solutions. Electrochemical impedance spectroscopy (EIS) was carried out on an Autolab potentiostat (Model PGSTAT302N) at room temperature in Ar purged solutions containing 0.0010 M equimolar concentrations of hexaminеruthenium(II) chloride and hexaminеruthenium(III) chloride, and 0.1 M KCl as supporting electrolyte. The formal potential (E_0') for the Ru(II)/Ru(III) redox couple was determined for each surface using cyclic voltammetry. Impedance spectra were performed at E_0' for

each surface; an equilibration time of 5 min at the applied potential was employed before each impedance measurement. The frequency response was recorded between 100 kHz and 0.1 Hz using a sinusoidal voltage with an amplitude of 10 mV. Equivalent electrical circuit modeling was performed using Nova (Version 1.8). Intercalation experiments were carried out in accordance with published methods,[12,14] via immersion of carbon substrates in 6×10^{-4} M acetonitrile solutions of 4NBA for 2 h. Samples were rinsed with abundant acetonitrile and dried under argon before cyclic voltammetry characterization.

3. Results

3.1 Properties of annealed amorphous carbon films

Amorphous carbon films (a-C) were deposited via DC magnetron sputtering as previously described.[12] These films had been shown to be semimetallic in character and to possess an sp^2 content of (80 ± 4)%, as determined via XPS.[12] a-C films were then annealed under a nitrogen atmosphere in order to increase their sp^2 carbon content. Figure 1a shows the Raman spectra of the as deposited a-C film, and of a-C after annealing at 500 °C (a-C500) and 700 °C (a-C700); the spectrum of glassy carbon (GC) is reported for comparison. All spectra show the characteristic D and G peaks of amorphous carbons.[16] Upon annealing, both D and G peaks become narrower, while the G peak also shifts towards higher wavenumbers; this is consistent with increasing sp^2 content and graphitization in the carbon film.[22,23] Peak fitting of spectra yielded I_D/I_G height ratios of 0.1, 0.5 and 0.7 for a-C, a-C500 and a-C700, respectively. Based on Ferrari's three-stage model for amorphous carbons, these ratios correspond to a change in sp^2 content from ~80% to ~100% upon annealing (see Supporting Information).[12,16] A qualitative comparison of the Raman spectrum of a-C700 to that of GC, a 100% sp^2 disordered carbon material, also suggests that a-C700 has ~100% sp^2 content.

The change in sp^2 content also affects the optical properties of a-C films. Figure 1b shows a 50 nm a-C film deposited on quartz before (left) and after (right) annealing at 700 °C, where the as prepared film displays greater transparency than the annealed one. The absorptivity of a-C films increased

significantly upon annealing as expected in the case of carbon graphitization.[22,24-26] Absorbance measurements were used to generate Tauc plots for annealed carbon films,[12,27] which yielded negative bandgap values for a-C700 of -0.8 eV (vs. 0.6 eV for a-C). Zero or negative Tauc gap values have been reported in the literature and are consistent with semimetallic electronic properties in deposited films.[28,29] An increase in the concentration of sp^2 bonded carbon upon annealing was also evident from X-ray photoelectron (XP) spectra; Figure 1c shows the C 1s spectrum of a-C and a-C700 surfaces. The main peak shifts to lower binding energies and becomes narrower after annealing at 700 °C, indicating a decrease in the contributions from sp^3 carbon centres.[30,31] Finally, the oxygen content of the carbon samples was found to decrease after annealing; analysis of O 1s peaks in a-C700 samples yielded an O/C ratio of 3%, lower than the 9% value observed for a-C surfaces.[12]

An increase in the concentration of sp^2 carbon centers is often accompanied by graphitization, whereby sp^2 centers organize into more and larger graphitic clusters. In order to obtain information on the relative density of graphitic edge planes exposed at the carbon surface before and after annealing, we carried out intercalation studies using 4-Nitrobenzylamine (4NBA), following methods developed by Compton and co-workers.[14] 4NBA has been shown to partially intercalate between exposed graphitic edge planes and the total charge associated to the electroreduction of intercalated nitroaryl groups to arylamines can be used to estimate the surface density of intercalation sites. Cyclic voltammetry of 4NBA-intercalated a-C700 samples was used in order to obtain the electroreduction charge (see Supporting Information), yielding a 4NBA surface density of $(19.5 \pm 1.8) \times 10^{-10}$ mol cm^{-2} (95% C.I.) This value suggests a significantly greater density of graphitic edge planes at annealed carbon surfaces when compared to the previously reported value for a-C of $(3.4 \pm 0.9) \times 10^{-10}$ mol cm^{-2} (95% C.I.).[12] Roughness measurements on a-C and a-C700 samples obtained via AFM also show that surface roughness is similar for these two samples; therefore, the observed difference in intercalated 4NBA surface densities cannot arise from differences in surface roughness (see Supporting Information). These results therefore indicate that both an increase in sp^2 carbon and graphitic clusters and edges take place

upon annealing; the effect of these changes on adsorption reactions will be discussed in the following section.

3.2 In situ and ex situ studies of 4NND and 5NND adsorption at amorphous carbon substrates

We carried out in situ spectroscopic studies of aryldiazonium adsorption at annealed carbon surfaces via Attenuated Total Internal Reflectance Fourier Transform Infrared Spectroscopy (ATR-FTIR), using 4NND and 5NND in solution. Carbon films were deposited and annealed at 700 °C onto a Si trapezoid; the trapezoid was incorporated into a flow cell for studying the carbon/solution interface in real time. Figure 2a shows an example of ATR-FTIR spectra in the region of the symmetric N—O stretching absorption over the course of a reaction; the peak is seen to increase during deposition. The net absorbance at 1342 cm^{-1}, after normalization by optical pathlength and absorption cross-section,[12,13] was used to provide a quantitative estimate of relative surface coverage for 4NND and 5NND vs. time, as previously described.[12,13] Previous work from our group on other aryldiazonium salts shows that surface coverage measured in situ contains contributions from both physisorbed and chemisorbed molecules; this is also true in the case of 4NND and 5NND adlayers, as shown in the Supporting Information.

Figure 2b shows adsorption curves for the two aryldiazonium isomers over 3 h of reaction time; the curves indicate that the two isomers display the same rate of adsorption at a-C700 surfaces. Similarly, no differences in morphology were observed when comparing 4NND and 5NND adlayers (see Supporting Information). This result is somewhat surprising given that 4NND is significantly easier to reduce than 5NND, with 4NND acceptor levels positioned 0.250 eV below those of 5NND.[13] This difference would suggest that adsorption rates should be larger for 4NND, as is indeed the case when adsorption rates are measured at as prepared a-C surfaces.[13] When comparing rates of adsorption at a-C vs. a-C700 we found that adsorption rates for 4NND increase slightly, whereas those of 5NND increase dramatically (see Figure 2c and 2d). Therefore, our results suggest that (a) the change in carbon composition/electronic properties upon annealing leads to an overall increase in reaction rates; (b) the

rate determining step of the 4NND grafting reaction might not depend on interfacial electron transfer rates.

In order to compare the behaviour observed at a-C700 carbon surfaces with that at a reference non-crystalline 100% sp^2 material, we carried out ex situ measurements at glassy carbon electrodes (GC) via electrochemistry. The integrated charge associated to the electroreduction of nitroaryl groups was obtained via cyclic voltammetry using samples prepared from 1×10^{-4} M aqueous solutions of 4NND and 5NND, after increasing reaction times. Figure 3a shows a typical cyclic voltammogram after deposition of 4NND and 5NND at GC electrodes; both peak potential and total charge associated to the reduction peak are similar for 4NND and 5NND adlayers. Figure 3b shows the surface density of nitroaryl groups at GC substrates obtained ex situ via this methodology vs. reaction time. Surface coverage in Figure 3b is seen to increase at similar rates for both molecules, measurements taken after 2 h of deposition (data not shown) indicate that the surface coverage levels off after 20 min. The limiting coverage was found to be 1.5×10^{-10} and 8.9×10^{-10} mol cm^{-2} for 4NND and 5NND, respectively, and slightly higher than a close-packed monolayer (1 ML = 6.01×10^{-10} mol/cm^2).[32] These results indicate that, although there is a difference in the limiting surface density of Ar-NO_2 in adlayers consisting of 4NND and 5NND at GC electrodes, the initial rate of adsorption of these two aryldiazonium cations is the same, in agreement with in situ measurements. Therefore, adsorption of the two positional isomers at GC as in the case of a-C700, is not controlled by the position of the molecular acceptor level.

3.3 Valence structure and electron transfer studies at amorphous carbons

The adsorption rate of aryldiazonium salts at carbon surfaces has been previously interpreted using the Marcus-Gerischer theory of charge transfer.[7] We were interested in understanding whether aryldiazonium cation adsorption at amorphous carbons could also be explained under the same theoretical framework. In order to do that we carried out experimental studies of the valence electronic

structure and of charge transfer rates at as prepared and annealed samples via Ultraviolet photoelectron spectroscopy (UPS) and electrochemical impedance spectroscopy (EIS).

The full UPS spectrum of a-C as deposited and after annealing shows broad features and poorly defined peaks characteristic of amorphous carbons (see Supporting Information).[33-35] Figure 4a shows the high-binding energy region of normalized UPS spectra of annealed a-C700 and as deposited a-C substrates. The high-binding energy emission threshold was fit to a line and extrapolated to the energy axis in order to calculate the high-binding energy cutoff value. This energy value was subtracted from the source photon energy (21.2 eV) to yield work function values of (4.2 ± 0.1) eV and (4.6 ± 0.1) eV for annealed a-C700 and as deposited a-C surfaces, respectively. The annealing treatment reduces the work function by 0.4 eV bringing its value close to that of 100% sp^2 glassy carbon (4.2 eV).[36] This indicates that the sputtered carbon sample undergoes graphitization, in agreement with Raman, UV and XPS results shown in Figure 1.

A decrease in work function after annealing is accompanied by an increase in photoelectron emission for energies near the Fermi energy (E_F), which can be observed in the low-binding region of the UPS spectra shown in Figure 4b. Marked enhancements in valence photoemission are observed for the annealed a-C700 film when compared to that of the as deposited a-C surface in the 0-4 eV region. This region is associated with contributions from p – π states in amorphous carbons and polycrystalline graphite.[33-35] The onset of photoemission approximately coincides with E_F in the case of a-C700, whereas for a-C the photoemission intensity is negligible (below noise equivalent level) in the region 0.19 eV-E_F; this suggests that a-C700 has a greater semimetallic character than a-C. Importantly, UPS results indicate that at the solid/vacuum interface, annealed a-C700 possesses higher lying occupied electronic states compared to pristine a-C.

The kinetics of electron transfer at the carbon/solution interface was investigated using EIS in solutions of $Ru(NH_3)_6^{+3/+2}$, a reversible redox couple with formal potential of E_0'= 0.034 V vs. SHE, at both amorphous carbon electrodes. Typical complex plane impedance (Nyquist) plots recorded for each carbon surface are shown in Figure 5. A modified Randles circuit, shown in the inset, was found to give

the best fit with an average χ^2 value of 0.05. In this equivalent circuit the resistance R_s represents the electrolyte resistance; the parallel combination of the constant phase element (CPE_p) and a resistance (R_{CT}) represent the double layer capacitance and the charge transfer resistance, respectively; finally, the Warburg element (W) models the diffusional impedance. Values of fitting parameters and details of the high frequency impedance are reported in the Supporting Information.

Figure 5 shows a large semicircular feature at high frequencies for as deposited a-C electrodes; this indicates that a significant charge transfer resistance, R_{CT} exists. The same feature is considerably smaller for annealed a-C700 electrodes, which display an impedance response dominated by the Warburg diffusional impedance. The Nyquist plot of a-C700 suggests that this material is highly graphitic and behaves similarly to 100% sp^2 glassy carbon electrodes, as shown in the Supporting Information. These results indicate that charge transfer rates for the $Ru(NH_3)_6^{+3/+2}$ couple are faster at a-C700 than at a-C electrodes. Using the values for R_{CT} obtained from the equivalent circuit fitting, the exchange current density (j_0) and thereby, the standard heterogeneous rate constant (k^0) could be calculated from equations (1-3):[37]

$$R_{CT} = \frac{RT}{Fj_0} \qquad (1)$$

$$i_0 = j_0 A = k^0 FCA \qquad (2)$$

$$k^0 = \frac{i_0}{FAC} \qquad (3)$$

Electron transfer heterogeneous rates constants k^0 were found to be 5.7×10^{-4} cm s^{-1} and 7.2×10^{-2} cm s^{-1} for a-C and a-C700 electrodes, respectively, in good agreement to previous determinations of k^0 for pyrolyzed photoresist film electrodes.[38,39] Importantly, these EIS results reveal a significant difference of two orders of magnitude in electron transfer rates at annealed a-C and as deposited a-C surfaces. In order to understand whether trends in electron transfer and in aryldiazonium interfacial adsorption can be explained by differences in electronic structure between these two carbon substrates, we analysed the

observed results under the framework of Marcus and Marcus-Gerischer theories of electron transfer as in the following section.

4. Discussion

Two amorphous carbon substrates that differ in graphitic content and two aryldiazonium cation isomers were used in this work in order to investigate interfacial reactivity trends. One of the carbon substrates, a-C, displays an estimated trigonally bonded carbon content of 80%, whereas the other one, a-C700, is 100% graphitic. The two aryldiazonium cations, shown in Scheme Ib are structural isomers, display the same surface geometric cross section but differ in the position of their electron acceptor level: 4NND is easier to reduce than 5NND by 250 mV, as shown in previous work (see Supporting Information).[13] This choice of molecules and substrates offers the opportunity to test some of the hypotheses advanced by us and others in the literature for the mechanism of spontaneous reactions of diazonium compounds at surfaces as well as for explaining the interfacial reactivity of amorphous carbon materials.

The amorphous carbon substrates examined, despite being both of high graphitic content, display marked differences in their electronic properties. The annealed sample, a-C700, has a negative Tauc gap which is characteristic of semimetallic materials; a-C samples, on the other hand, have a small but finite Tauc gap. The semimetallic character of a-C700 and the presence of a small optical gap in a-C are consistent with UPS measurements which indicate that the onset of emission for a-C700 coincides with E_F whereas in the case of a-C it is positioned ~0.2 eV below E_F. UPS measurements also show that (a) the intensity of photoemission in the 4-0 eV binding energy region is higher and (b) that the work function is lower for a-C700 than for a-C. UPS results therefore indicate that based on thermodynamics arguments, a-C700 should behave as a better electron donor in charge transfer reactions because it possesses higher lying donor states than a-C.

Electrochemical impedance measurements also indicate that the kinetics of electron transfer is faster at a-C700 than at a-C surfaces. The electron transfer rate constant (k^0) for $Ru(NH_3)_6^{+3/+2}$ was found to be 126 times higher for a-C700 relative to a-C. Given that $Ru(NH_3)_6^{+3/+2}$ is an outer-sphere redox couple

that has been shown to be rather insensitive to surface sites but sensitive to the density of states (DOS) of carbon electrodes,[40] it is interesting to interpret observed differences in k^0 on the basis of DOS differences near the Fermi level of these two carbon materials. Theories of charge transfer have been successfully used in the recent literature to model electron transfer rates obtained from electrochemical measurements at carbon electrodes. For instance, Compton and co-workers have used Marcus-Hush theory to relate electron transfer rates to the DOS of a graphite microelectrode;[41] Heller et al.[42] and Szroeder et al.[43,44] have used Gerischer-Marcus (GM) theory in order to model electron transfer rates based on the DOS distribution of carbon nanotube electrodes. Gerischer-Marcus theory has also been used to interpret and model spontaneous electron transfer from graphene nanoribbons and carbon nanotubes to aryldiazonium cations.[6,7] Therefore, in our analysis we decided to use GM theory in order to discuss under the same framework both EIS findings and spontaneous reactions of aryldiazonium at amorphous carbon electrodes.

GM theory considers that electron transfer rates depend on the overlap between occupied donor and unoccupied acceptor states. For electron transfer from the electrode to an oxidized species in solution, the electron transfer rate at energy E is proportional to the number of unoccupied states in solution $W_{ox}(E)$, and to the number of occupied states at the electrode $DOS_{occ}(E)$, where $DOS_{occ}(E)$ depends on the applied electrode potential. The total electron transfer rate constant, k_r, is proportional to the overlap integral over all possible energies:[7,43]

$$k_r \propto \int_{-\infty}^{+\infty} DOS_{occ}(E) W_{ox}(E) dE \qquad (4)$$

The energy distribution of states in solution is assumed to be a Gaussian:[37]

$$W_{ox}(E) = \frac{1}{\sqrt{4\pi\lambda kT}} \exp\left(- \frac{\left(E - \left(\lambda + E_{redox}\right)\right)^2}{4\pi\lambda kT} \right) \qquad (5)$$

where k is Boltzmann's constant, T is temperature, λ is the reorganization energy and E_{redox} is the redox potential of the species in solution.

Assuming that the proportionality pre-factor is the same for both a-C700 and a-C substrates, equation (4) allows us to estimate the relative values of electron transfer rate constants for $Ru(NH_3)_6^{+3/+2}$ from the occupied density of states in order to compare it to experimentally determined rate constants. In order to use equation (4) to model relative electron transfer rates at amorphous carbons it is necessary to obtain the density of occupied states, $DOS_{occ}(E)$. The UPS photoemission intensity can be used for this purpose; however, obtaining the $DOS_{occ}(E)$ would require to correct the UPS spectra by the photoemission cross section.[45,46] If only the photoemission intensity over a narrow energy range within few eV of the Fermi level is used, we can assume that changes in cross section over this energy range are small so that the cross section can be included in the proportionality factor. Furthermore, if interested in relative values of rate constants, we can assume that photoemission cross sections are similar for both a-C and a-C700; this approximation is reasonable given that in this region the majority of photoelectrons originate from similar p-π states in both graphitic materials.[45] Using these assumptions, we can approximate the ratio between the electron transfer rate constants of a-C and a-C700 for spontaneous reductions as:

$$\frac{k_{r,aC}}{k_{r,aC700}} \cong \frac{\int_{E_{\min}}^{E_F} I_{aC}(E) W_{ox}(E) d\varepsilon}{\int_{E_{\min}}^{E_F} I_{aC700}(E) W_{ox}(E) d\varepsilon} \qquad (6)$$

where $I_{aC}(E)$ and $I_{aC700}(E)$ are the photoemission intensities of a-C and a-C700 surfaces, respectively, and $[E_{min}\,;\,E_F]$ defines an energy integration interval over occupied states at the electrode for which the overlap with acceptor states in solution is non-negligible (vide infra).

EIS measurements using $Ru(NH_3)_6^{+3/+2}$ were carried out at the formal potential, E_0', of the redox couple. Figure 6 shows the energy positions of the Fermi levels of carbon surfaces and redox species used in our experiments relative to vacuum; redox potentials were positioned with respect to vacuum using the absolute potential scale derived by Trasatti.[47] The figure shows that a negative potential of ~100 mV and a positive potential of ~300 mV must be applied to a-C and a-C700 electrodes, respectively, in order to bring their Fermi levels to coincide with E_0'. The density of occupied states $DOS_{occ}(E)$ depends

on the applied potential; however, on a first approximation we can assume that whenever a small potential is applied to our carbon electrodes it is dropped primarily over the double layer. Therefore, upon applying a potential all valence band states simply shift in energy while maintaining the position of the Fermi level fixed with respect to band edges. This approximation is justifiable and less stringent than it would first appear, since amorphous carbons are rich in localized states and defects, which result in pinning of the Fermi level as shown for instance by Miyajima et al.[46] and Ilie et al.[48]

Under the above approximations it is possible to calculate the ratio of electron transfer rate constants by integrating the overlap of the photoemission intensity and the acceptor state distribution after alignment of the Fermi levels. Figure 7 shows an example of this procedure in the case of a-C and $Ru(NH_3)_6^{+3/+2}$: the $W_{ox}(E)$ distribution was calculated according to equation (5), assuming room temperature and a reorganization energy of 0.8 eV, as determined by Smalley et al. at gold electrodes.[49] The integral can then be calculated over a limited energy range over which the overlap is significant, as shown in the inset of Figure 7. Following the above procedure we calculated the ratio of the overlap integrals between the normalized photoemission curves of a-C and a-C700 and the acceptor level distribution function of $Ru(NH_3)_6^{+3/+2}$ calculated by (5). The GM prediction for the ratio $k_{r,aC} : k_{r,\ aC700}$ is 1 : 82, in good agreement with the ratio of 1 : 126 measured via EIS. This result suggests that the approximation described by equation (4) offers a good approach for estimating relative charge transfer rate constant values at amorphous carbon electrodes.

The same procedure was used to estimate the rates of electron transfer to aryldiazonium cations in solution. The distributions of acceptor levels $W_{ox,4NND}(E)$ and $W_{ox,5NND}(E)$ were calculated using equation (5), previously determined values of E_{redox},[13] and λ=0.7 eV, a value obtained by Nair et al.[6] by fitting kinetic data on the spontaneous reactions of a phenyldiazonium cations at carbon nanotubes to the GM model. Using equation (6) we then calculated the relative values of reduction rate constants for 4NND and 5NND at both a-C and a-C700 samples, which are summarized in Table 1. It is clear from the values in Table 1 that for an electron transfer mediated reaction step GM theory predicts faster reaction rates for 4NND than for 5NND, and for a-C700 than for a-C, under the same conditions.

If the initial adsorption rate were exclusively controlled by an electron transfer step, relative adsorption rates would be expected to be comparable to GM model predictions; in fact, the GM model appears to be a good approach for predicting relative charge transfer rates for the $Ru(NH_3)_6^{+3/+2}$ redox couple in solution. Results in Table 1 are in qualitative agreement with our observation of faster adsorption rates of 5NND at a-C700 vs. a-C surfaces in situ (see Figure 2d). However, the observed relative adsorption rates for 5NND at time zero on these two surfaces differ by much less than the 5 orders of magnitude predicted by GM models. Strikingly, the GM model predicts approximately a 20-fold difference for electron transfer from a-C700 to 4NND and 5NND; in contrast, in situ adsorption data in Figure 2b and ex situ chemisorption data in Figure 3b show little or no difference between 4NND and 5NND reaction rates at 100% sp^2 amorphous carbons. Finally, in situ adsorption data for 4NND at a-C and a-C700 surfaces yields only very small differences in the rate of adsorption (Figure 2c), whereas the GM model estimates a difference of 3 orders of magnitude.

The fact that, compared to GM model predictions, smaller or no differences are observed experimentally among adsorption rates might be explained by two possible arguments: (a) differences in adsorption rate at annealed surfaces are below what can be distinguished via our experimental method; (b) the overall aryldiazonium cation adsorption process is controlled by steps that follow the initial electron transfer-mediated adsorption (step 1 in Scheme 1). The first hypothesis appears unlikely, given that the expected differences are extremely large. The second hypothesis appears instead to be likely, based on previous literature on carbon nanotube reactions by Strano and co-workers. Nair et al.,[6] in fact, observed a similar effect in the kinetic selectivity of aryldiazonium grafting towards metallic and semiconducting nanotubes; at high aryldiazonium salt concentrations the first adsorption step becomes non-limiting and therefore the reaction rate becomes independent of the carbon substrate electronic properties. In previous work from our group we found that the early aryldiazonium adsorption curves could be easily modeled using reversible Langmuir adsorption at amorphous carbon surfaces that are poor electron donors (H-doped carbon), however, it was not possible to use the same model for more graphitic surfaces.[21] The current results as well as our previous work therefore suggest that although electron-

transfer is important for the first adsorption step, there must exist a threshold rate of electron transfer beyond which adsorption is determined by other processes. For instance, surface diffusion or reorientation of aryldiazonium adsorbates might be necessary in order to chemisorb aryldiazonium adsorbates through nitrogen elimination. Also and importantly, in order for the reaction to proceed and yield a chemisorbed species it is necessary to preserve charge neutrality, as suggested by experimental evidence by Downard and co-workers;[50] reaction of the surface with hole scavengers must therefore occur in parallel to aryldiazonium reduction and can potentially control reaction rates.

5. Conclusions

Amorphous carbons offer an interesting opportunity for improving our understanding of reactions at carbon materials since it is possible to modulate their electronic and optical properties to examine their effect on surface chemistry. We have used Gerischer-Marcus theory in order to interpret experimentally determined charge transfer rates and aryldiazonium cation adsorption results. GM theory was successful at predicting relative charge transfer rates at graphitic amorphous carbon surfaces under the assumptions outlined in the Discussion section: predicted rates were found to be of the same order of magnitude and within 30% of the experimentally determined values. To our knowledge, this is the first example of a successful correlation between valence electronic structure determinations and electrochemical electron transfer rate results at amorphous carbon materials.

The same GM model was applied to spontaneous aryldiazonium cation adsorption; however, we found that GM predicted much larger differences in adsorption rates than those observed experimentally. This suggests that electron transfer mediated adsorption of aryldiazonium cations at graphitic amorphous carbons is fast to the point that they become not rate-determining, even at early reaction times.

This result has important implications in order to understand (1) the chemistry of amorphous carbon materials and (2) surface functionalization reactions using aryldiazonium salts. A first conclusion is that it appears possible to apply theories of charge transfer that have worked in the past for materials with long range order (e.g. gold, graphene, nanotubes) also to these disordered materials with high density of

localized states and defects. A second conclusion is that, although the rate of spontaneous reduction is a good criterion to estimate relative rates of aryldiazonium adsorption at carbons, once the electron transfer rate is sufficiently fast the reaction is controlled by other processes. Although at this stage we can only speculate on the identity of these processes, possible steps could be, for instance, hole scavenging at the carbon or surface reorientation and/or diffusion. Finally and importantly, our results show how a controlled change in carbon composition can be used to gain mechanistic insights on chemical reactions and to develop guiding criteria for achieving selectivity in interfacial reactions.

Acknowledgements. This publication has emanated from research conducted with the financial support of Science Foundation Ireland under Grant Number 09/RFP/CAP2174. R.D. and M.E.G.L. also acknowledge support from Science Foundation Ireland under Grant Number SFI/10/IN.1/I2969.

Supporting Information Available. D/G ratios obtained via Raman, Tauc plots of amorphous carbon samples, cyclic voltammetry of electrodes intercalated with 4-nitrobenzylamine, AFM characterization of surfaces, XPS characterization of adlayers, full UPS spectra of carbon surfaces and EIS of annealed a-C700 and glassy carbon electrodes, summary table of redox potentials. This material is available free of charge via the Internet at http://pubs.acs.org.

References

(1) Paulus, G. L. C.; Wang, Q. H.; Strano, M. S. Covalent Electron Transfer Chemistry of Graphene with Diazonium Salts. *Acc. Chem. Res.* **2012**, *46*, 160-170.

(2) Mahouche-Chergui, S.; Gam-Derouich, S.; Mangeney, C.; Chehimi, M. M. Aryl Diazonium Salts: A New Class of Coupling Agents for Bonding Polymers, Biomacromolecules and Nanoparticles to Surfaces. *Chem. Soc. Rev.* **2011**, *40*, 4143-4166.

(3) Belanger, D.; Pinson, J. Electrografting: A Powerful Method for Surface Modification. *Chem. Soc. Rev.* **2011**, *40*, 3995-4048.

(4) Barrière, F.; Downard, A. Covalent Modification of Graphitic Carbon Substrates by Non-Electrochemical Methods. *J. Solid State Electrochem.* **2008**, *12*, 1231-1244.

(5) Pinson, J.; Podvorica, F. Attachment of Organic Layers to Conductive or Semiconductive Surfaces by Reduction of Diazonium Salts. *Chem. Soc. Rev.* **2005**, *36*, 429-439.

(6) Nair, N.; Kim, W.-J.; Usrey, M. L.; Strano, M. S. A Structure-Reactivity Relationship for Single Walled Carbon Nanotubes Reacting with 4-Hydroxybenzene Diazonium Salt. *J. Am. Chem. Soc.* **2007**, *129*, 3946-3954.

(7) Sharma, R.; Nair, N.; Strano, M. S. Structure-Reactivity Relationships for Graphene Nanoribbons. *J. Phys. Chem. C* **2009**, *113*, 14771-14777.

(8) Strano, M. S.; Dyke, C. A.; Usrey, M. L.; Barone, P. W.; Allen, M. J.; Shan, H.; Kittrell, C.; Hauge, R. H.; Tour, J. M.; Smalley, R. E. Electronic Structure Control of Single-Walled Carbon Nanotube Functionalization. *Science* **2003**, *301*, 1519-1522.

(9) Usrey, M. L.; Lippmann, E. S.; Strano, M. S. Evidence for a Two-Step Mechanism in Electronically Selective Single-Walled Carbon Nanotube Reactions. *J. Am. Chem. Soc.* **2005**, *127*, 16129-16135.

(10) Baik, S.; Usrey, M.; Rotkina, L.; Strano, M. S. Using the Selective Functionalization of Metallic Single-Walled Carbon Nanotubes to Control Dielectrophoretic Mobility. *J. Phys. Chem. B* **2004**, *108*, 15560-15564.

(11) Kim, W. J.; Usrey, M. L.; Strano, M. S. Selective Functionalization and Free Solution Electrophoresis of Single-Walled Carbon Nanotubes: Separate Enrichment of Metallic and Semiconducting Swnt. *Chem. Mater.* **2007**, *19*, 1571-1576.

(12) Cullen, R. J.; Jayasundara, D.; Soldi, L.; Cheng, J.; DuFaure, G.; Colavita, P. E. Spontaneous Grafting of Nitrophenyl Groups on Amorphous Carbon Thin Films: A Structure-Reactivity Investigation. *Chem. Mater.* **2012**, *24*, 1031–1040.

(13) Murphy, D. M.; Cullen, R. J.; Jayasundara, D. R.; Scanlan, E. M.; Colavita, P. E. Study of the Spontaneous Attachment of Polycyclic Aryldiazonium Salts onto Amorphous Carbon Substrates. *RSC Advances* **2012**, *2*, 6527–6534.

(14) Wildgoose, G. G.; Wilkins, S. J.; Williams, G. R.; France, R. R.; Carnahan, D. L.; Jiang, L.; Jones, T. G. J.; Compton, R. G. Graphite Powder and Multiwalled Carbon Nanotubes Chemically Modified with 4-Nitrobenzylamine. *ChemPhysChem* **2005**, *6*, 352-362.

(15) Kiema, G. K.; Aktay, M.; McDermott, M. T. Preparation of Reproducible Glassy Carbon Electrodes by Removal of Polishing Impurities. *J. Electroanal. Chem.* **2003**, *540*, 7-15.

(16) Ferrari, A. C.; Robertson, J. Interpretation of Raman Spectra of Disordered and Amorphous Carbon. *Phys. Rev. B* **2000**, *61*, 14095-14107.

(17) Colavita, P. E.; Sun, B.; Tse, K. Y.; Hamers, R. J. Photochemical Grafting of N-Alkenes onto Carbon Surfaces: The Role of Photoelectron Ejection. *J. Am. Chem. Soc.* **2007**, *129*, 13554-13565.

(18) Díaz, J.; Paolicelli, G.; Ferrer, S.; Comin, F. Separation of the Sp^3 and Sp^2 Components in the C 1s Photoemission Spectra of Amorphous Carbon Films. *Phys. Rev. B* **1996**, *54*, 8064-8069.

(19) Ertl, G.; Küppers, J. *Low Energy Electrons and Surface Chemistry*; Wiley-VCH: Weinheim, 1986.

(20) Schlaf, R.; Schroeder, P. G.; Nelson, M. W.; Parkinson, B. A.; Lee, P. A.; Nebesny, K. W.; Armstrong, N. R. Observation of Strong Band Bending in Perylene Tetracarboxylic Dianhydride Thin Films Grown on Sns2. *J. Appl. Phys.* **1999**, *86*, 1499-1509.

(21) Jayasundara, D.; Cullen, R. J.; Colavita, P. E. In Situ and Real Time Characterization of Spontaneous Grafting of Aryldiazonium Salts at Carbon Surfaces. *Chem. Mater.* **2013**, *25*, 1144–1152.

(22) Wang, T. M.; Wang, W. J.; Chen, B. L.; Zhang, S. H. Electrical and Optical Properties and Structural Changes of Diamondlike Carbon Films During Thermal Annealing. *Phys. Rev. B* **1994**, *50*, 5587-5589.

(23) Noguchi, T.; Shimada, T.; Chiba, T.; Terada, M.; Hasegawa, T. Very High Temperature Annealing Effect on Amorphous Carbon Films Grown on Refractory Oxide Substrates by Pulsed Laser Deposition. *Diamond Relat. Mater.* **2010**, *19*, 107-109.

(24) Fanchini, G.; Tagliaferro, A. Localisation and Density of States in Amorphous Carbon-Based Alloys. *Diamond Relat. Mater.* **2001**, *10*, 191-199.

(25) Foulani, A. Annealing Effects on Optical and Photoluminescence Properties of a-C : H Films. *J. Phys. D: Appl. Phys.* **2003**, *36*, 394.

(26) Robertson, J. Diamond-Like Amorphous Carbon. *Mater. Sci. Eng. R* **2002**, *37*, 129-281.

(27) Sun, B.; Colavita, P. E.; Kim, H.; Lockett, M.; Marcus, M. S.; Smith, L. M.; Hamers, R. J. Covalent Photochemical Functionalization of Amorphous Carbon Thin Films for Integrated Real-Time Biosensing. *Langmuir* **2006**, *22*, 9598-9605.

(28) Fendrych, F.; Pajasova, L.; Wagner, T.; Jastrabik, L.; Chvostova, D.; Soukup, L.; Rusnak, K. Cnx Coatings Sputtered by Dc Magnetron: Hardness, Nitrogenation and Optical Properties. *Diamond Relat. Mater.* **1999**, *8*, 1711-1714.

(29) Faizrakhmanov, I.; Bazarov, V.; Stepanov, A.; Khaibullin, I. Modification of the Nanostructure of Diamond-Like Carbon Films by Bombardment with Xenon Ions. *Semiconductors* **2003**, *37*, 723-726.

(30) Haerle, R.; Riedo, E.; Pasquarello, A.; Baldereschi, A. Sp^2/Sp^3 Hybridization Ratio in Amorphous Carbon from C 1s Core-Level Shifts: X-Ray Photoelectron Spectroscopy and First-Principles Calculation. *Phys. Rev. B* **2001**, *65*, 045101.

(31) Jackson, S. T.; Nuzzo, R. G. Determining Hybridization Differences for Amorphous Carbon from the Xps C 1s Envelope. *Appl. Surf. Sci.* **1995**, *90*, 195-203.

(32) Hallmark, V. M.; Chiang, S.; Brown, J. K.; Wöll, C. Real-Space Imaging of the Molecular Organization of Naphthalene on Pt(111). *Phys. Rev. Lett.* **1991**, *66*, 48-51.

(33) Reinke, P.; Oelhafen, P. Thermally Induced Structural Changes in Amorphous Carbon Films Observed with Ultraviolet Photoelectron Spectroscopy. *J. Appl. Phys.* **1997**, *81*, 2396-2399.

(34) Schelz, S.; Richmond, T.; Kania, P.; Oelhafen, P.; Güntherodt, H.-J. Electronic and Atomic Structure of Evaporated Carbon Films. *Surf. Sci.* **1996**, *359*, 227-236.

(35) McFeely, F. R.; Kowalczyk, S. P.; Ley, L.; Cavell, R. G.; Pollak, R. A.; Shirley, D. A. X-Ray Photoemission Studies of Diamond, Graphite, and Glassy Carbon Valence Bands. *Phys. Rev. B* **1974**, *9*, 5268-5278.

(36) Kelemen, S. R.; Freund, H.; Mims, C. A. The Interaction of Koh with Clean and Oxidized Carbon Surfaces. *J. Catal.* **1986**, *97*, 228-239.

(37) Bard, A. J.; Faulkner, L. R. *Electrochemical Methods: Fundamentals and Applications*, 2nd ed.; John Wiley & Sons: New York, 2001.

(38) Fairman, C.; Yu, S. C.; Liu, G.; Downard, A.; Hibbert, D. B.; Gooding, J. J. Exploration of Variables in the Fabrication of Pyrolysed Photoresist. *J. Solid State Electrochem.* **2008**, *12*, 1357-1365.

(39) Ranganathan, S.; McCreery, R. L. Electroanalytical Performance of Carbon Films with near-Atomic Flatness. *Anal. Chem.* **2001**, *73*, 893-900.

(40) McCreery, R. L. Advanced Carbon Electrode Materials for Molecular Electrochemistry. *Chem. Rev.* **2008**, *108*, 42.

(41) Nissim, R.; Batchelor-McAuley, C.; Henstridge, M. C.; Compton, R. G. Electrode Kinetics at Carbon Electrodes and the Density of Electronic States. *Chem. Commun.* **2012**, *48*, 3294-3296.

(42) Heller, I.; Kong, J.; Williams, K. A.; Dekker, C.; Lemay, S. G. Electrochemistry at Single-Walled Carbon Nanotubes: The Role of Band Structure and Quantum Capacitance. *J. Am. Chem. Soc.* **2006**, *128*, 7353-7359.

(43) Szroeder, P. Electron Transfer Kinetics at Single-Walled Carbon Nanotube Paper: The Role of Band Structure. *Physica E* **2011**, *44*, 470-475.

(44) Szroeder, P.; Tsierkezos, N. G.; Scharff, P.; Ritter, U. Electrocatalytic Properties of Carbon Nanotube Carpets Grown on Si-Wafers. *Carbon* **2010**, *48*, 4489-4496.

(45) Schäfer, J.; Ristein, J.; Graupner, R.; Ley, L.; Stephan, U.; Frauenheim, T.; Veerasamy, V. S.; Amaratunga, G. A. J.; Weiler, M.; Ehrhardt, H. Photoemission Study of Amorphous Carbon Modifications and Comparison with Calculated Densities of States. *Phys. Rev. B* **1996**, *53*, 7762-7774.

(46) Miyajima, Y.; Tison, Y.; Giusca, C. E.; Stolojan, V.; Watanabe, H.; Habuchi, H.; Henley, S. J.; Shannon, J. M.; Silva, S. R. P. Probing the Band Structure of Hydrogen-Free Amorphous Carbon and the Effect of Nitrogen Incorporation. *Carbon* **2011**, *49*, 5229-5238.

(47) Trasatti, S. The Concept of Absolute Electrode Potential an Attempt at a Calculation. *J. Electroanal. Chem.* **1974**, *52*, 313-329.

(48) Ilie, A.; Hart, A.; Flewitt, A. J.; Robertson, J.; Milne, W. I. Effect of Work Function and Surface Microstructure on Field Emission of Tetrahedral Amorphous Carbon. *J. Appl. Phys.* **2000**, *88*, 6002-6010.

(49) Smalley, J. F.; Finklea, H. O.; Chidsey, C. E. D.; Linford, M. R.; Creager, S. E.; Ferraris, J. P.; Chalfant, K.; Zawodzinsk, T.; Feldberg, S. W.; Newton, M. D. Heterogeneous Electron-Transfer Kinetics for Ruthenium and Ferrocene Redox Moieties through Alkanethiol Monolayers on Gold. *J. Am. Chem. Soc.* **2003**, *125*, 2004-2013.

(50) Lehr, J.; Williamson, B. E.; Downard, A. J. Spontaneous Grafting of Nitrophenyl Groups to Planar Glassy Carbon Substrates: Evidence for Two Mechanisms. *J. Phys. Chem. C* **2011**, *115*, 6629-6634.

Tables

	Relative values of electron transfer rate constants	
	a-C	**a-C700**
4NND	355	1.8×10^6
5NND	1	1.0×10^5

Table 1. Relative values of electron transfer rate constants for the spontaneous reduction of aryldiazonium cations in water at the two carbon surfaces investigated in this work, calculated using a Gerischer-Marcus model and equation (6) in the text.

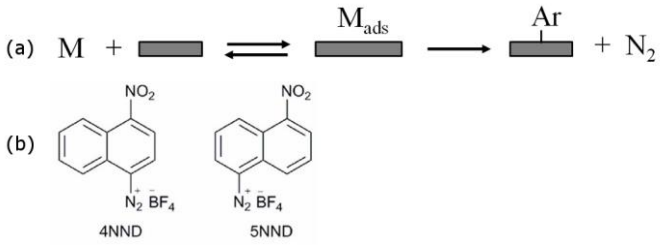

Scheme I: (a) Proposed mechanism of aryldiazonium salt chemisorption reactions. (b) Molecules used in our experiments.

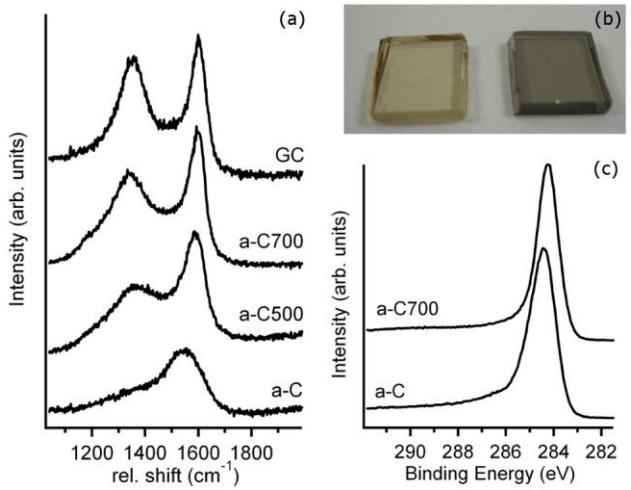

Figure 1. (a) Raman spectra (514 nm) of carbon films as deposited (a-C), after annealing at 500 °C (a-C500), at 700 °C (a-C700), and of glassy carbon (GC). (b) a-C deposited on quartz before (left) and after (right) annealing at 700 °C. (c) C 1s XP spectra of a-C and a-C700 films.

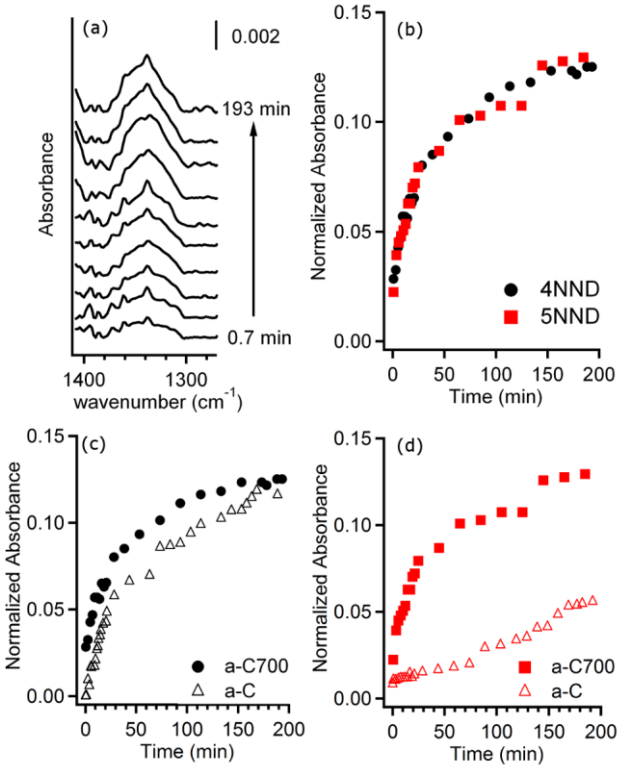

Figure 2. (a) Symmetric -NO_2 stretching peak of 4NND obtained via in situ ATR-FTIR at a-C700 surfaces after injection of 1×10^{-4} M 4NND. (b) Adsorption curves for 4NND and 5NND at a-C700, after normalization. Comparison of adsorption curves of 4NND (c) and 5NND (d) at a-C and a-C700 obtained from 1×10^{-4} M solutions over 3 h of reaction.

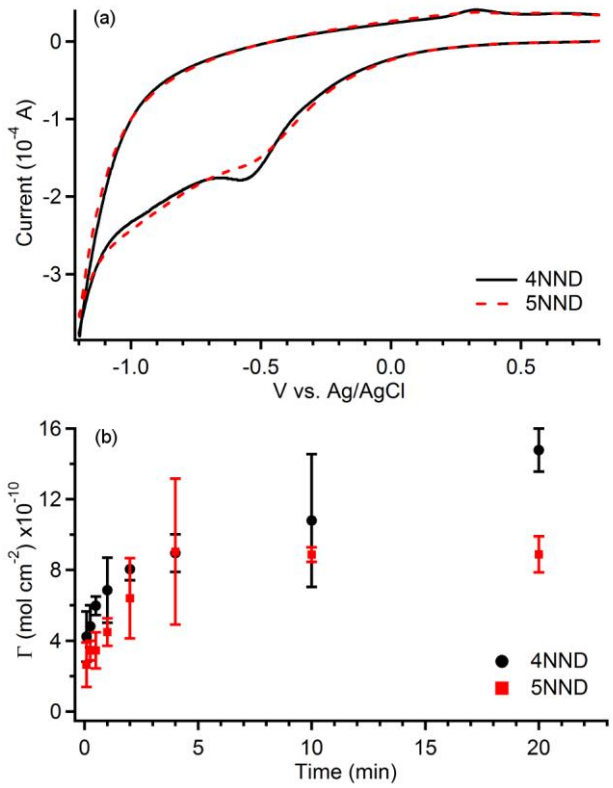

Figure 3. (a) Cyclic voltammograms of 4NND and 5NND-modified GC electrodes obtained in 0.1 M H_2SO_4 at 0.2 V s^{-1}; substrates were modified by immersion in 1×10^{-4} M aqueous solutions of 4NND and 5NND for 10 min. (b) Surface coverage of nitroaryl groups (Γ) on GC substrates as a function of deposition time in 1×10^{-4} M 4NND (●) and 5NND (■) aqueous solutions.

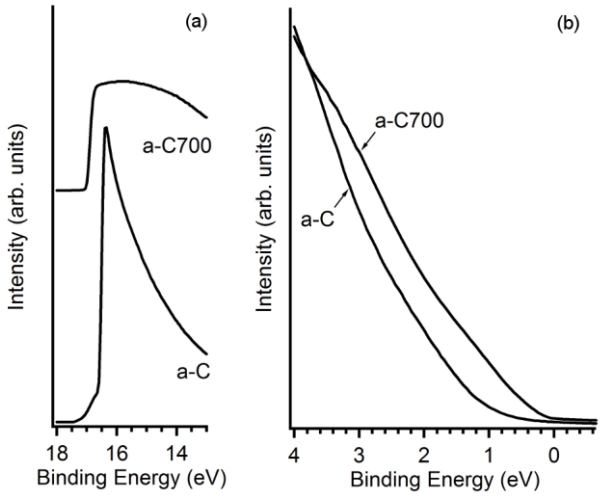

Figure 4. (a) High and (b) low binding energy regions of normalized UPS spectra of annealed carbon (a-C700) and as deposited amorphous carbon (a-C) surfaces.

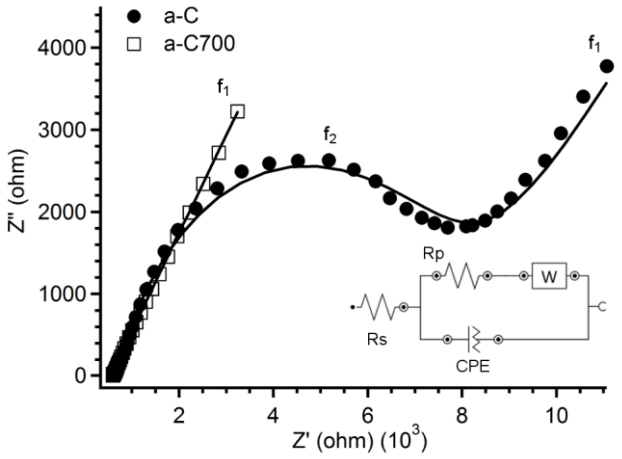

Figure 5. Experimental impedance data represented as Nyquist plots for a-C and annealed a-C700 electrodes. Continuous lines show the best fit of EIS data using the equivalent circuit shown in the inset; frequencies at maximum Z" are f_1 = 0.100 Hz and f_2 = 16.000 Hz.

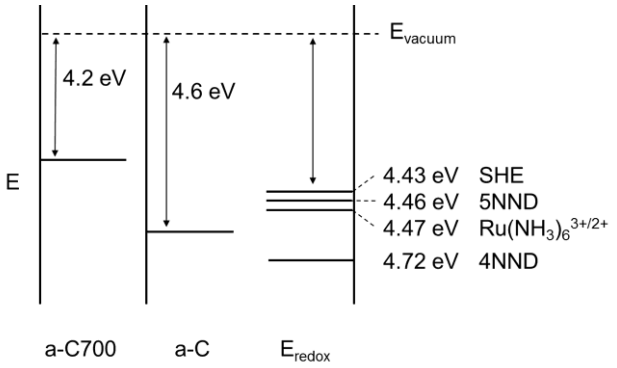

Figure 6. Scheme showing the Fermi levels obtained from work function determinations of carbon substrates in this manuscript, the position of electron acceptor levels of 4NND and 5NND obtained from electrochemical measurements,[13] and the literature position of the Standard Hydrogen Electrode (SHE), all relative to vacuum.[47]

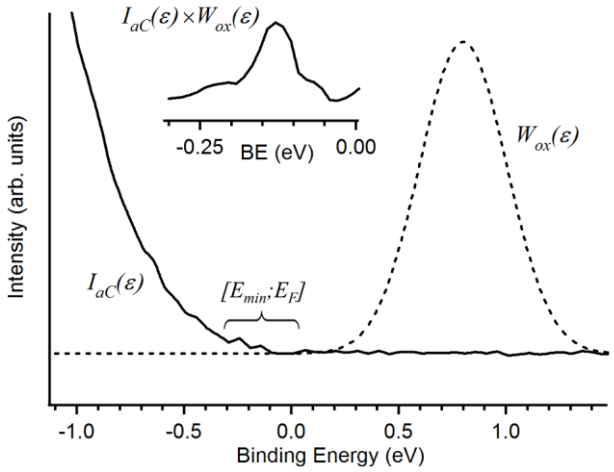

Figure 7. Example of the integration procedure used to calculate charge transfer rate constant ratios using the approximation in equation (6). The intensity of the UPS photoemission and the distribution of $Ru(NH_3)_6^{+3/+2}$ acceptor levels in solution are shown after alignment of their Fermi levels (E=0); the y-scaling is arbitrarily chosen for the two curves in order to facilitate graphical comparison. The inset shows the product of the two curves which defines a narrow energy interval over which the overlap can be integrated (indicated by the bracket).

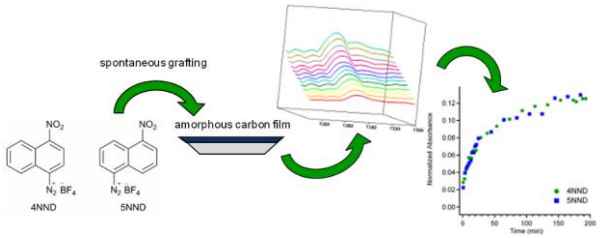
spontaneous grafting
amorphous carbon film
4NND
5NND
Time (min)
4NND
5NND

ToC Graphic.